MICROSTRUCTURE AND PHYSICAL PROPERTIES OF MnZn FERRITES FOR THE HIGH FREQUENCY POWER SUPPLIES

M. Drofenik
Jožef Stefan Institute, Ljubljana, Slovenia

INVITED PAPER
33rd International Conference on Microelectronics,
Devices and Materials, MIDEM´97
September 24. - September 26., 1997, Hotel Špik, Gozd Martuljek, Slovenia

Keywords: MnZn ferrites, microstructure properties, physical properties, power suplies, high frequency power supplies, grain sizes, grain boundary properties, power losses, magnetic losses, high electrical resistance, aliovalent ions, ion doping, oxygen concentration, SMPS, switch-mode power supplies, eddy current

Abstract: The power loss of MnZn ferrites and its relation to the average grain size and grain boundary properties was studied. It was found that the power loss depend on the average grain size and on the highly electrically resistive grain boundaries which are formed by introduction of aliovalent ions in the intrinsic grain boundary of MnZn ferrite grains. A lower concentration of oxygen during sintering decreases the average grain size and improves the magnetic loss.

Mikrostrukturne in fizikalne lastnosti MnZn feritov za uporabo v visokofrekvenčnih napajalnikih

Ključne besede: MnZn-feriti, lastnosti mikrostrukturne, lastnosti fizikalne, napajalniki energetski, napajalniki energetski visokofrekvenčni, velikost zrn, lastnosti zrn mejne, izgube močnostne, izgube magnetne, upornost električna visoka, ioni aliovalentni, dopiranje ionov, koncentracija kisika, SMPS napajalniki komutacijski, tok vrtinčni

Povzetek: Preučevali smo močnostne izgube MnZn feritov in odvisnost izgub od povprečne velikosti zrn in lastnosti meja med zrni. Ugotovili smo, da je izguba odvisna tako od povprečne velikosti zrn, kakor tudi od mej med zrni z izredno visoko električno upornostjo, ki jih ustvarimo z vgradnjo večvalentnih ionov v zrna MnZn ferita. Nižja koncentracija kisika med sintranjem zmanjša povprečno velikost zrn in izboljša magnetne izgube.

1. INTRODUCTION

The application of MnZn ferrites in power electronics is constantly increasing. Particularly the growth of the commercial market for Switch Mode Power Supplies (SMPS) places demands on the ferrite industry to produce high performance ferrite cores capable of operating at increasingly higher frequencies /1/. In SMPS the switching frequency is related to the power output, making it possible for smaller core volumes to transform the same amount of power as a larger core would at lower frequencies. This is a direct challenge for the miniaturization of SMPS and related power devices /2/.

The main core characteristics are core losses which contribute the major part of the total electrical loss. In general the core loss can be divided into a residual loss, a hysteresis loss and an eddy current loss. The residual loss is important only at low induction levels and can be ignored in the power application of MnZn ferrites. The hysteresis loss $P_H = W_h f$, where $W_H = \int HdB$ is the energy represented by the area of the hysteresis loop measured under the maximum flux density, depends on many parameters; however, hindrance to domain wall displacements /3/, which takes place at high induction levels /4/, plays the major role.

The factors governing the hysteresis loss are the magnetocrystalline anisotropy K_1 magnetostriction λ, stress σ, porosity p, and saturation magnetization M_S. For low hysteresis loss K_1, λ, σ, and p should be low. These parameters can be controlled by the chemical composition; however, the porosity (p) and mechanical stress (σ) are controlled mostly by the microstructure and impurities. The ferrous content, which is essential in MnZn ferrites for achieving low magnetisation anisotropy and magnetostriction and thus low hysteresis loss, gives rise to a high electrical conductivity due to the thermally activated hopping mechanism between Fe^{2+} and Fe^{3+} in spinel ferrites. The relatively low electrical resistivity, ρ_{bulk}, influences the eddy current loss, $P_E = AB_m^2 f^2 / \rho_{bulk}$, where A is the core cross section, Bm is the maximal flux density, and f is the frequency. The most effective way to suppress electron hopping and thus the electrical conductivity inside the ferrite grains, is by the substitution of Ti^{4+}, which occupies the B site /5/ adjacent to Fe^{2+}.

At higher operating frequencies the contribution of the eddy current loss to the total loss strongly increases and above 500 kHz it dominates all other losses. Therefore in order to increase the performance of MnZn ferrites for powder applications at higher frequencies, the eddy current losses must be suppressed to the greatest possible extent.

2. CORRELATION BETWEEN MICROSTRUCTURE PARAMETERS AND POWER LOSS

In MnZn ferrites the grain boundary shows different chemical and physical properties from the ferrite grains. The segregation of impurities and partial reoxidation of Fe^{2+} on the grain boundaries during cooling makes the MnZn ferrite grain boundaries highly insulating in comparison to the grain interior. These insulating layers are in practice very thin and therefore exhibit a relatively high electrical capacity.

For such a ferrite core the equivalent electrical circuit of the semiconducting grains and the insulating grain boundaries form a resistance and capacitance connected in parallel whose impedance causes a dispersion with respect to the frequency /6/.

The impedance of parallel R;C; elements, which usually represent the equivalent circuit of a MnZn ferrite, is

$Z = Z' - jZ''$ where

$$Z' = \sum \frac{R_i}{1+(\omega R_i C_i)^2} \quad \text{and} \quad Z'' = \sum R_i \frac{\omega R_i C_i}{1+(\omega R_i C_i)^2}.$$

The impedance

$$Z = \sqrt{(Z')^2 + (Z'')^2}$$

for $\omega RC << 1$ where $\omega = 2\pi f$ will be close to the pure ohmic resistance $Z \rightarrow R$. However, in the case when $\omega RC >> 1$ and consequently $Z \rightarrow 1/\omega C$ the grain boundary capacitance will play the dominant role in the MnZn ferrite. Thus, depending on the operating frequency, two extreme cases govern the impedance of the MnZn ferrite and its power losses.

In order to elucidate the dependence of power loss P on the average grain size D and the grain boundary thickness δ_{gr} and its resistance R_{gr} which are the essential microstructure element, we will divide the ferrite material into small cubes, i.e. the brick wall model, Fig. 1. In this hypothetical model the grain boundaries with a thickness $\delta_{g.b.}$ will lie in directions perpendicular and parallel to the principal axis, i.e. to the electric field direction. The grain boundaries which are parallel to the principal axis will be electrically bypassed by the bulk material. Therefore the small cubes can be approximated by bulk material separated by high ohmic layers - the grain boundaries which are perpendicular to the principal axis. Each layer can be represented by a resistance-capacitance (R - C) lumped circuit of high ohmic layers. When the resistivity of the bulk is much lower than the grain boundary layers, the equivalent circuit of the ferrite can be represented by a series of lumped R - C circuits of the grain boundary layers.

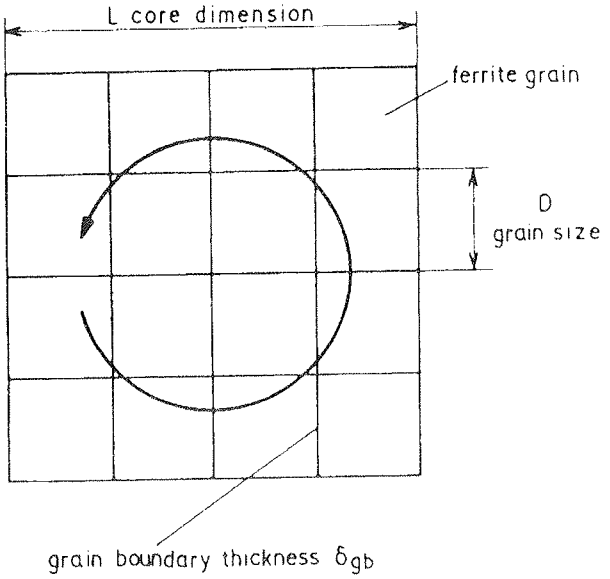

Fig.1: Brick wall microstructure model: a sketch of an ideal microstructure of a material - MnZn ferrite - with grain boundaries permeable to the eddy current

In a real material, the grains have the shapes of irregular polyhedra. In this case only the components of the grain boundaries which are perpendicular to the principal axis can effectively block the electric current.

By applying this model /7/ the macroscopic resistance, which can be obtained from the impedance spectra, can be expressed as

$$R_{g.b.}^{(mac.)} = R_{g.b.}^{(mic.)} \cdot \frac{L}{D+\delta_{g.b.}} \quad \text{where} \quad \frac{L}{D+\delta_{g.b.}} \approx \frac{L}{D}$$

is the number of grain boundaries perpendicular to the electric field, $\delta_{g.b.}$ is thickness of the grain boundary,

$$R_{g.b.}^{(mac.)} = \rho_{g.b.}^{(mic.)} \cdot \frac{L}{A}$$

is the macroscopic resistance obtained from complex impedance plots and L/A is length-area ratio of the samples. Further, by combination of the above Eqs. it follows that

$$\rho_{g.b.}^{(mac.)} = R_{g.b.}^{(mic.)} \cdot \frac{A}{D} = \rho_{g.b.}^{(mic.)} \frac{\delta_{g.b.}}{D}.$$

When we combine this expression with that of the eddy current loss, we finally obtain

$$P_e = cB_m^2 f^2 \cdot \frac{D}{R_{g.b.}^{(mic)}} \qquad (1)$$

Thus, at lower frequencies $\omega RC << 1$, the eddy current is proportional to the average grain size and inversely to the resistance of a grain boundary $R_{g.b.}^{(mic)}$. On the other hand, at higher frequencies where $\omega RC >> 1$ when again applying the brick-wall model, where for each grain boundary intersection perpendicular to the electric field

$$C^{(mic)} = \varepsilon_o \cdot \varepsilon_{g.b.} \frac{A}{\delta_{g.b.}}$$

and considering the number of grain boundaries $\approx L/D$, then it follows that

$$\frac{1}{C^{(mac)}} = \frac{L}{D}\frac{1}{C^{(mic)}} \quad \text{and finally} \quad C^{(mac)} = \varepsilon_o \cdot \varepsilon_{g.b.} \frac{D}{\delta_{g.b.}}\frac{A}{L}$$

By inserting the impedance in the relation for the eddy current power loss we obtain

$$P_E \approx cAB_m^2 f^2 \times \omega C^{(mac)} \propto \varepsilon_{g.b.} \frac{D}{\delta_{g.b.}} \qquad (2)$$

We can see that when $\omega RC >> 1$ the eddy current loss is determined by the average grain size, the thickness of the grain boundary and its permittivity. Therefore from the above considerations it can be seen that the average grain size is to a great extent the dominant microstructural parameter in the whole frequency range and determines the eddy current loss. Further, we can see that up to the operating frequencies where the grain boundaries are not short circuited by a high displacement current, the power loss of MnZn ferrites can be effectively suppressed by a decrease in average grain size $\overline{D}$, by increasing the grain boundary resistance $R_{g.b.}^{(mic)}$, by increasing the grain boundary width $\delta_{g.b.}$ and/or bydecreasing its permittivity $\varepsilon_{g.b.}$

3. TAILORING OF MICROSTRUCTURE PARAMETERS AND POWER LOSSES

The average grain size of a MnZn ferrite can be effectively decreased by sintering it at a lower oxygen partial pressure /8/, while the grain boundary resistivity can be increased by the addition of aliovalent ions to the ferrite /9/.

In order to engineer the MnZn ferrite parameters, i.e. to decrease average grain size (D) and/or to increase the intrinsic grain boundary resistance, the concentration of oxygen during sintering may be varied from 21 vol. % to 1 vol. % and the ferrite should be doped with aliovalent ions which segregate to the grain boundary during sintering.

It is well established that a higher amount of oxygen 21 vol. % increases the pore mobility and induces exaggerated pore growth, while a lower concentration of oxygen increases the concentration of the slowest moving species, i.e. oxygen vacancies, and promotes volume diffusion and hence grain boundary mobility /10/. On the other hand, the pore - grain boundary interaction during sintering has a decisive influence on the microstructure /11/. Depending on the pore size/grain size ratio, the grain growth is largely determined by the attachment or separation of the pores from the grain boundary. When this ratio is small the pores will be left behind and the conditions for the formation of grains with exaggerated grain size and trapped pores will be present. So, if one would like to engineer effectively the MnZn ferrites microstructure, exaggerated pores must first be developed by using a high partial pressure of oxygen during sintering. If these pores are large enough they can effectively pin the grain boundaries /12/ and impede grain growth at lower $P(O_2)$ (if applied) which promotes densification and grain boundary mobility.

Fig. 2 shows a typical power loss dependence vs. the temperature of MnZn ferrites sintered at different partial pressures of oxygen /8/ (sample 1 sintered at 21 vol% of oxygen, sample 2 at 10 vol % of oxygen, sample 3 at 5 vol % and the sample 4 at 1 vol % of oxygen). The essential microstructural parameters of the samples are shown in Table I.

Table I: The key microstructural parameters of the sintered samples; density (ρ), percentage of theoretical density (TD), average grain size ($\overline{D}$), average grain size without giant grains ($\overline{D}'$), and percentage of giant grains (A).

Sample code	ρ [g/cm^3]	TD Š%]	$\overline{D}$ [μm]	$\overline{D}'$ [μm]	A* [%]
1	4.88	95	10.87	-	-
2	4.90	96	9.95	9.87	8
3	4.93	97	9.36	9.19	6
4	4.94	97	9.54	9.20	14

* grains with more than two trapped pores

The density of the samples is more or less the same, with the exception of sample 1 which has a lower density. On the other hand, the average grain size and the percentage of grains with exaggerated grain size and intragranular porosity is different. The nominal composition of the samples studied is the same and can be excluded from further consideration. The outstanding properties of samples 2 and 3 can therefore be assigned exclusively to the influence of sample microstructure and their stoichiometry.

In the case that the operating frequency is lower than the relaxation frequency of the wall displacement, hysteresis and eddy current losses prevail. The equation which relates the static permeability (μ_s), relaxation frequency (f_r) and microstructural parameter (D) is $f_r(\mu_s - 1) = 3/4\ (4\pi Ms)2/\pi zD$, where Ms is the saturation magnetisation /13/. In Fig. 3 the permeability spectra of the high frequency power ferrites are shown.

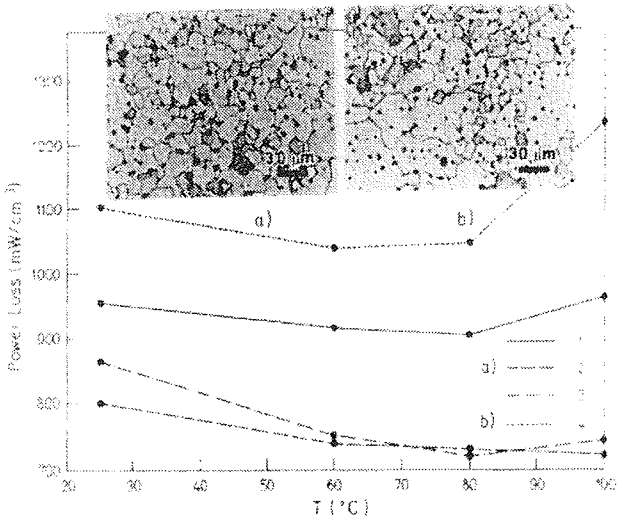

Fig. 2: Temperature dependence of core loss at 700 kHz (50 mT) for samples sintered at 1280°C and 21 vol % oxygen (sample 1),10 vol % (sample 2), 5% (sample 3) and 1 vol % of oxygen for sample 1 respectively and typical microstructures; a) sample 2 and b) sample 4.

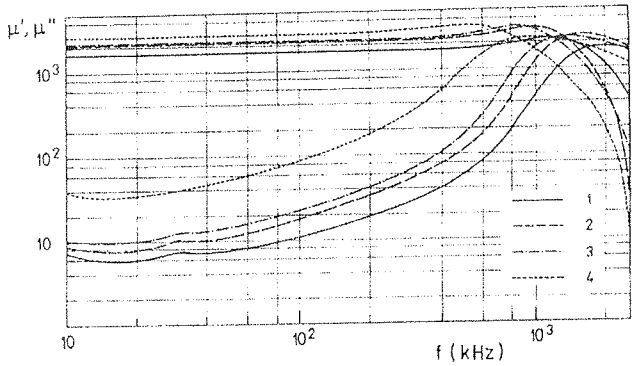

Fig. 3: Permeability spectra of high frequency MnZn-power ferrites for samples 1, 2, 3, and 4.

Table II: Permeability spectra of samples studied; relaxation frequency (f_r), static permeability (μ_s), the product ($f_r \cdot \mu_s$), the product, ($f_r \cdot \mu_s \cdot D$), and the amount of FeO present in the samples

Sample code	f_r [MHz]	μ_s -	$f_r \cdot \mu_s$ [GHz]	$f_r \cdot \mu_s \cdot D$ [KHzm]	[FeO] [%]
1	2.0	1800	3.6	39.6	2.15
2	1.8	2400	4.3	40.3	2.41
3	1.4	2500	3.5	32.76	2.48
4	1.0	3000	3.0	28.62	2.68

The values of the products $fr\ \mu s\ \overline{D} \equiv A$ in Table I, which is proportional to $M_s^2/ß$, gradually decrease indicating that the dumping ability of samples increases with the concentration of Fe^{2+} ions. All samples contain an equal amount of the four-valent ions Ti^{4+} and Sn^{4+} which when dissolved in the ferrite grains produce about 0.74 wt. % FeO. The rest is formed during the sintering at equilibrium conditions due to dissolution of the excess iron oxide in the spinel lattice and is $P(O_2)$ dependent. This part of the FeO and/or Fe^{2+} is not localised in Fe^{2+}-$Ti^{4+}(Sn^{4+})$ pairs and contributes to the damping mechanism, and thus decreases the relaxation frequency. In Fig. 4 the relationship between core loss per cycle (P/f) and the frequency is shown. A linear relationship was clearly found for all samples in accordance with the general expression for power loss

$$P/f = A + Cf \quad \text{where} \quad A = \int HdB, C = aB_m^2/\rho_{bulk} \propto D/\delta_{gr}$$

The eddy current loss of the samples, the grain resistivity and the grain boundary resistivity are given in Table III.

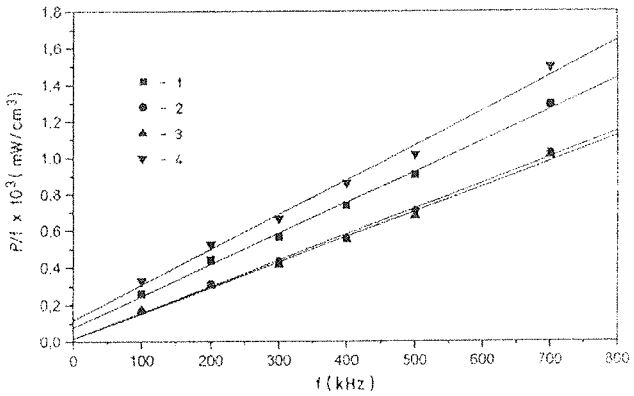

Fig. 4: Power loss per frequency vs. frequency for samples 1, 2, 3, and 4

Table III: Grain resistivity, grain boundary resistivity and eddy current losses at 80°C measured at 700 kHz (50 mT).

Sample code	Grain resistivity [Ω cm]	Grain bound. resistivity [Ω cm]	$P_E^{80°C}$ [mW/cm³]
1	7	63	833
2	8	64	686
3	7	66	686
4	7	22	931

Samples 1 and 4 show larger eddy current losses compared to the other two samples.

The eddy current loss depends mainly on the bulk electrical resistivity of the samples. The resistivity of a polycrystalline ferrite can be increased by increasing its grain boundary resistivity and/or reducing the grain size. At constant grain boundary resistance, the bulk resistance can be increased by reducing the average grain size and/or by increasing the number of grain boundaries $R_{bulk} = R_g + R_{g.b.}$. Samples 2, 3 and 4 exhibit smaller average grain size in comparison to sample 1 and therefore lower P_E losses. Sample 4 is an exception where the fraction of giant grains is relatively high. A higher fraction of these grains can substantially decrease the number of grain boundaries per eddy current path. On the other hand, in sample 1 neither are giant grains developed, nor is the grain boundary resistivity significantly lower. Besides, sample 1 has a higher total porosity which can create a demagnetisation field, a lower μ, and a substantial increase of the magnetic flux density and lead to an increase of the total loss. When considering grain boundary properties in electrical ceramics, AC impedance methods are widely used for their characterisation. When the experimental data are analysed and interpreted it is essential to have a model equivalent circuit that provides an acceptable representation of the electrical properties. In the MnZn ferrite ceramics considered it is well known that both inter- and intragranular impedances are present.

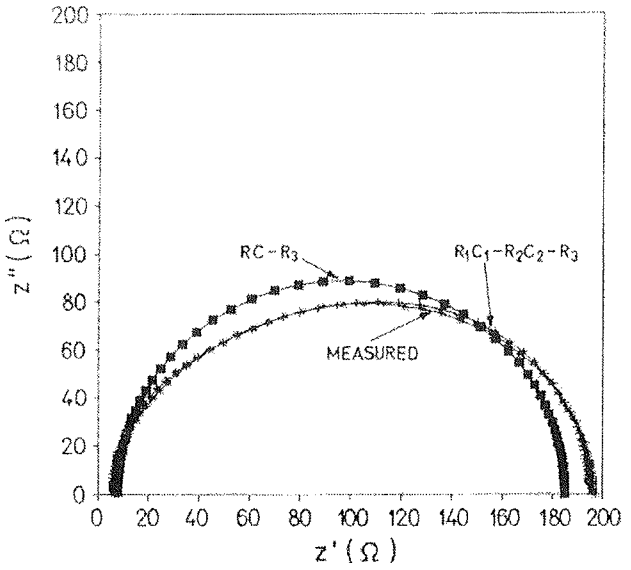

Fig. 5: Measured complex impedance spectra of doped MnZn ferrite sample doped with 0.2 wt% Ta_2O_3 sample with a fitted spectra with single RC value for the grain boundary and a fitted spectra in which the distinction is made between the extrinsic and intrinsic grain boundary.

In Fig. 5 a typical complex impedance spectrum is shown for the doped ferrite samples and a corresponding simulated spectrum when the distinction is made between an extrinsic and an intrinsic grain boundary, i.e. R_1C_1-R_2C_2-R_3. In addition, a simulated impedance spectrum where a single R and C value, i.e. RC-R_3 was used to fit the spectrum is also shown. Fig. 5 indicates that a simulated impedance spectrum where the grain boundary is separated fits the experimental measurements much better than those where a single RC element is used. This confirms that the separation of the grain boundary into an intrinsic and extrinsic part seems to be justified.

The electrical properties are determined in general by a series combination of such impedances which can be represented by a parallel RC element. From the complex impedance spectra of doped and undoped samples and the corresponding simulated impedance spectra, parallel R_1C_1-R_2C_2-R_3 elements were obtained. Once the equivalent circuits and corresponding elements of the circuits are obtained, these elements must be assigned to the microstructural characteristics of the material, provided that the measured response belongs entirely to the sample.

In the case where one would like to estimate the dimension and/or volume of a particular component in a sample using capacitance data, the permittivity of the region considered must be known. The samples studied are ferromagnetic and not ferroelectric, with a permittivity like that of an oxide, $\varepsilon = 10$. From the relation $C = \varepsilon_0 A/L$ a unit volume of such a material would have a capacitance of about 1 pF. Experimental data for capacitance C measured at 10 kHz for the samples studied were in the range from 3.2×10^{-6} to 4.2×10^{-7}F. Assuming A is unity, the thickness of this region must be reduced

$$\delta_{g.b.} = A\frac{\varepsilon}{C(pF)} = 3 - 21\,nm.$$

The capacitance is associated with thin non-ferroelectric regions, as indicated by their large capacitance value of a few μF, and these regions are therefore assigned to MnZn ferrite grain boundaries. According to the data obtained by fitting the measured data by an equivalent circuit, it is suggested that beside the extrinsic grain boundary a highly resistive surface layer on each MnZn ferrite grain can be present as well. The AC impedance spectra of the MnZn ferrite samples studied suggests that the electrical make-up of the MnZn ferrite ceramics is as shown in Fig. 6.

The resistances R_1, R_2 and R_3, representing the appropriate electrical elements (RC), must be related to the electrical scheme in Fig 6. R_3 can be assigned to the grain resistance due to the relatively low value of R_3, in accordance with the basic electrical properties of MnZn ferrite grains. On the other hand, R_1 and R_2 are related to the grain boundary and must therefore be assigned to the "extrinsic" grain boundary due to second phase formation at the boundaries, and to the "intrinsic" grain boundary due to the segregation effect.

In ferrites the basic electron conduction mechanisms have been studied by many investigators and reviewed by Klinger et al. /14/. Various models were proposed; however, the thermally activated hopping model has been shown to be appropriate in explaining qualitatively the electrical behavior of MnZn ferrites. The additional

electron on a ferrous (Fe^{2+}) ion requires little energy to move to an adjacent (Fe^{3+}) on the equivalent lattice sites (B sites). Under the influence of the electric field, these extra electrons hopping between iron ions constitute the electrical conduction. Therefore, any change in the divalent iron ion content in the spinel ferrite lattice and/or the distance between them is crucial to the intrinsic resistivity of MnZn ferrite grains, including the intrinsic grain boundaries.

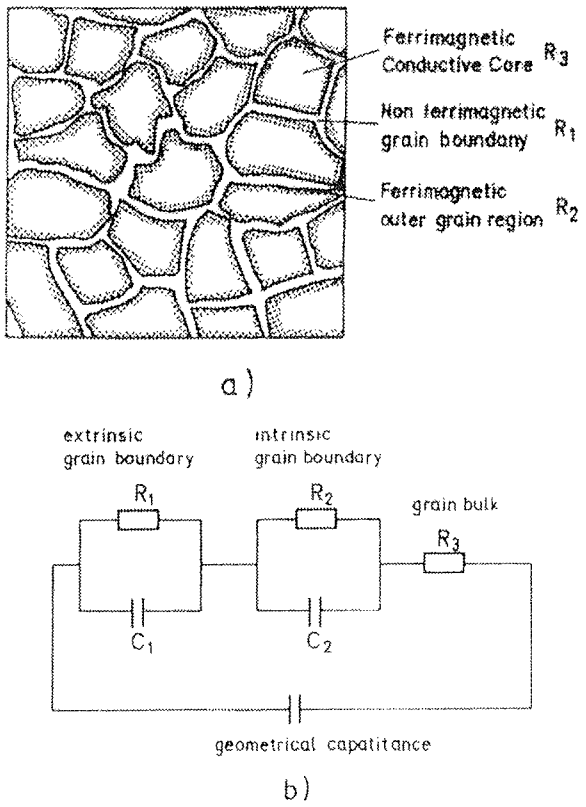

Fig. 6: Schematic model representing the electrical make-up: a) of polycrystalline MnZn ferrite; R_1-non ferrimagnetic grain boundary, R_2-ferrimagnetic outer grain region, R_3-ferrimagnetic conductive core b) the corresponding equivalent circuit.

If the introduction of another cation into the lattice causes a change in the valency distribution on the B-sites, then the number of electrons potentially available for transfer will be altered. On the other hand, the incorporation of foreign ions can change the distance between the B lattice-sites, which is crucial for the conduction mechanism. Thus, the formation of an "intrinsic" grain boundary in doped samples by the segregation of aliovalent ions must increase the intrincic grain boundary resistivity very much.

Due to their specific properties the grain boundaries are prone to the segregation of impurities. The driving forces for equilibrium segregation in ceramics are elastic and electrostatic interactions between segregation species in the bulk and in the interfacial region. The most important process occurring on the grain boundaries of MnZn ferrites during sintering are the segregation of aliovalent ions /15/, and Zn depletion /16/, caused by grain boundary diffusion of Zn to the surface of the sample and evaporation of ZnO from the sample surface. Besides, any change in the Fe/O ratio is usually identified on the grain boundary of MnZn ferrite grains.

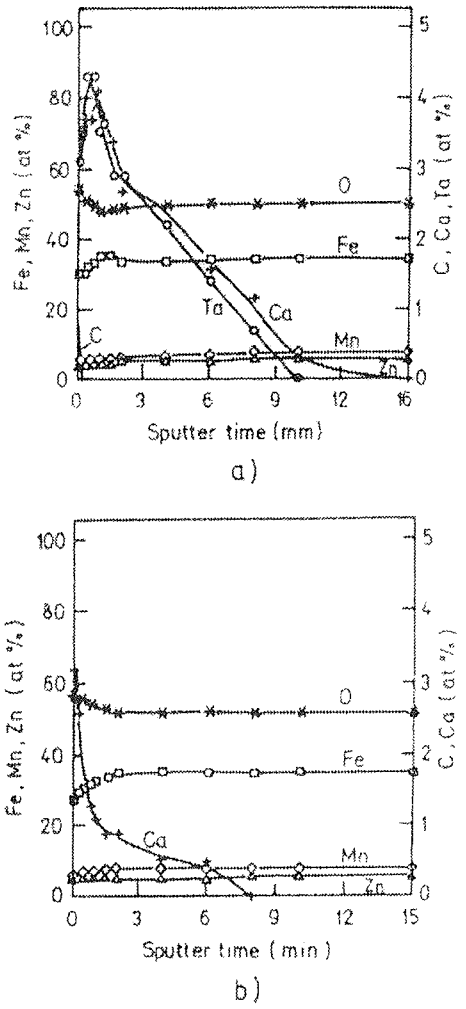

Fig.7(a,b): A typical AES concentration depth profile of MnZn ferrite grain boundaries containing Ta^{3+} dopants and Ca^{2+} impurities; Fig. 7a concentration depth profile of samples doped with Ta^{3+} ions and b) undoped sample where only impurities of Ca^{2+} ions can be identified

Extensive grain boundary analyses of MnZn ferrites were performed in the past /17,18/ where the grain boundary composition in the outer layer of MnZn ferrite grains was considered. Our results for grain boundary analyses are consistent with those previously reported. A decrease of the Fe/O ratio and a depletion of Zn was detected on the grain boundary of the samples analyzed. The segregation of Ca, which is an impurity, can be detected usually in ferrite samples exhibiting improved high frequency magnetic properties /19/ Figs. 7(a,b). In samples doped with Ta_2O_5 the segregation of Ta was confirmed, Fig. 7a. The Auger Electronic Spectra of fractured grain boundary surfaces showed the presence of a concentration depth profile of the aliovalent

ions Ca^{2+} and Ta^{5+} in the outer layer of the MnZn ferrite grains, and thus confirm the presence of an intrinsic grain boundary present in MnZn ferrite grains as identified by complex impedance spectra of ferrites studied.

5. FINAL REMARKS

Results reveal that the essential parameters which determine the P_E loss of MnZn ferrites in the frequency range up to 1 MHz are exclusively average grain size, grain boundary thickness and its resistance. Thus, when engineering the high frequency properties of MnZn ferrite the complex composition of the intrinsic grain boundary must be controlled in order to decrease the eddy current loss at high frequencies.

6. REFERENCES

/1/ A. Goldman, "Modern Ferrite Technology", Van Nostrand Reinhold, N. Y.1990.

/2/ C. R. Hendricks, V. W. R. Amarakoon, "Processing of MnZn Ferrites for HighFrequency Switch-Mode Power Supplies", Cer. Bull., 70(5), (1991) 817-23.

/3/ M. Guyot and A. Globus, "Determination of the Domain Wall Energy and the Exchange Constant from Hysteresis in Ferromagnetic Polycrystals", J. Phys., Supp. 38(4), (1977) 157-68.

/4/ J. Smit and H. P. J. Wijn, Ferrites, Phil. Tech. Library, Eindhoven 1959.

/5/ T.G. Stijntjes, J. Klerk, A. B. Groenou, "Permeability and Conductivity of Ti-Substitute MnZn Ferrites", Philips Res. Rep., 25, (1970) 95-107.

/6/ C.G. Koops, "On the Dispersion of Resistivity and Dielectric Constant of Some Semiconductors at Audiofrequencies", Phys. Rev. 84(1),121-124 (1951).

/7/ P.J. Van Dijk, A.J. Burggraaf, "Grain Boundary Effects on Ionic Conductivity in Ceramics $Gd_xZ_{1-x}O_{2-x}/2$ Solid Solutions", Phys. Stat. Sol. (a) 63, 229-241 (1981).

/8/ A. Žnidaršič, M. Drofenik, "Influence of Oxygen Partial Pressure During Sintering on the Power Loss of MnZn Ferrites", IEEE Trans. Mag 32(3),1941-1945 (1996).

/9/ A. Žnidaršič, M. Limpel, M. Drofenik, "Effect of Dopants on the Magnetic Properties of MnZn Ferrites for High Frequency Power Supplies", IEEE Trans. Mag. 31(2), 950-953 (1995).

/10/ P.J.L. Reijnen, "Sintering Behaviour and Microstructures of Aluminates and Ferrites with Spinel Structure with Regard to Deviation from Stoichiometry", Science of Ceramics, 4, (1968) 169-188.

/11/ R.J. Brook, "Pore - Grain Boundary Interaction and Grain Growth", J. Am. Cer. Soc., 52 (1), (1969) 56-57.

/12/ F.M.A. Carpy, "The Effect of Pore Drag on Ceramic Microstructures", Ceramic Microstructures, 76, Ed. R. M. Fulrath and J. A. Pash, Colorado (1977) pp. 261-275.

/13/ M. Guyot and V. Cagan, "Temperature Dependence of the Domain Wall Mobility in YIG deduced from Frequency Spectra of the Initial Susceptibility of Polycrystals" J. Mag. Mag. Mat., 27, (1982) 202-208.

/14/ M.I. Klinger and A.A. Samokhvalov, "Electron Conduction in Magnetite and Ferrites", Phys. Stat. Sol. (b) .79, 9-48 (1977).

/15/ A. Nakata, H. Chihara and A. Sasaki, "Microscopic Study of Grain-Boundary Region in Polycrystalline Ferrites", J. Appl. Phys. 57 (1), 4177-4179 (1985).

/16/ J. Van der Zaag, J.J.M. Ruigrok, A. Noordermeer, M.H.W.M. van Delden, P.T. Por, M.Th. Rekveldt, D. M. Donnet and J.N. Chapman, "The Initial Permeability of Polycrystalline MnZn Ferrites: The Influence of Domains and Microstructure", J. Appl. Phys. 74 (6), 4085-4095 (1993).

/17/ P.E.C. Franken and W.T. Stacy, "Examination of Gran Boundaries of Mn-Zn Ferrites by AES and TEM", J. Am. Cer. Soc. 63 (5-6), 315-319 (1980).

/18/ M. Drofenik, S. Beseničar, M. Limpel and V. Gardaševič, "Influence of the Dimension of MnZn Ferrite Samples on their Microstructural and Magnetic Properties", pp. 229-235 in Advances in Ceramics, Vol. 16, Ed. F.F.Y. Wang, The Am. Cer. Soc., Inc., Columbus, OH 1985.

/19/ M. Drofenik, A Žnidaršič, I. Zajc, "High Resistive Grain Boundaries in Doped MnZn Ferrites for High Frequency Power Supplies", J. Appl. Phys. 82(1), 333 - 340 (1997)

Prof. dr. M. Drofenik, dipl.ing.
Jožef Stefan Institute,
Jamova 39,1001 Ljubljana, Slovenia,
miha.drofenik @ijs.si

Prispelo (Arrived): 15.09.1997 *Sprejeto (Accepted): 09.12.1997*